NARLabs National Applied Research Laboratories

N S P O

Multiphysics Modeling of Rocket Combustion

Yen-Sen Chen

National Space Organization, Hsinchu, Taiwan

S.S. Wei, Alfred Lai, J.W. Lin, T.H. Chou, J. S. Wu

Dept. of Mech. Engr., National Chiao Tung Univ., Hsinchu, Taiwan

ICPFDS 2014, Nov. 25-27, 2014, NTU, Taipei, Taiwan

Happy Birthday Tony !!!

Outline

- Introduction
- Numerical Approach
  - All-Speed Flow Solver
  - Real-Fluid Properties
  - Combustion Models with Finite-rate Chemistry
  - Fluid-Structure Interaction Modeling
- Numerical Model Validations
- Rocket Engine Design Applications
- Conclusions

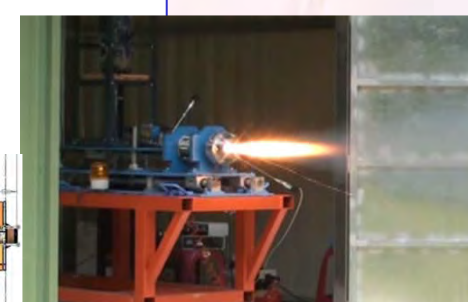

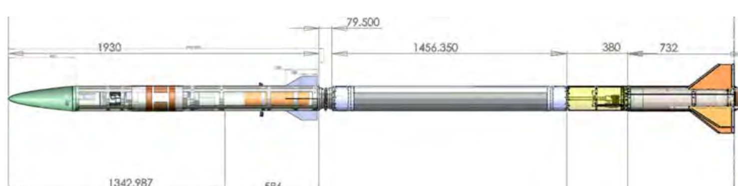

Introduction

- Rocket propulsion technology/performance drives space exploration and science missions
- Liquid, solid and hybrid rocket propulsion involves complex physics & flow operating conditions
- Computational modeling – an cost-effective design approach in modern propulsion system developments for combustion efficiency optimization and system integrity verification
- Very useful diagnostic tool in hot-fire experimental investigations
- Critical design analysis issues:
  - Real-fluid properties (suitable for sub- and super-critical combustion conditions)
  - Accurate transient reacting flow with high fidelity thermal modeling
  - Realistic flexible wall boundaries – fluid-structure interactions

Numerical Approach

- Governing Equations: Navier-Stokes with turbulence, finite-rate chemistry, real-fluid, particulate two-phase flow, radiation models
- Pressure-based all-speed formulation with unstructured grid finite-volume method and parallel computing capability
- Transient rocket engine flow validated and developing fluid-structure interaction capabilities

Flow Solver Governing Equations

$$
\left\{
\begin{array}{l}
\dfrac{\partial \rho}{\partial t}+\dfrac{\partial}{\partial x_j}(\rho V_j)=0 \\[2ex]
\dfrac{\partial(\rho V_i)}{\partial t}+\dfrac{\partial}{\partial x_j}(\rho V_j V_i)=-\dfrac{\partial p}{\partial x_i}+\dfrac{\partial \tau_{ji}}{\partial x_j}+S_V \qquad ; \qquad \tau_{ji}=(\mu+\mu_t)\left(\dfrac{\partial V_i}{\partial x_j}+\dfrac{\partial V_j}{\partial x_i}-\dfrac{2}{3}\dfrac{\partial V_k}{\partial x_k}\delta_{ij}\right) \\[2ex]
\dfrac{\partial(\rho h_t)}{\partial t}+\dfrac{\partial}{\partial x_j}(\rho V_j h_t)=\dfrac{\partial p}{\partial t}+\dfrac{\partial}{\partial x_j}\left[\left(\dfrac{\mu}{\mathrm{Pr}}+\dfrac{\mu_t}{\mathrm{Pr}_t}\right)\dfrac{\partial h_t}{\partial x_j}\right]-\dfrac{\partial}{\partial x_j}\left[\left(\dfrac{\mu}{\mathrm{Pr}}+\dfrac{\mu_t}{\mathrm{Pr}_t}\right)\dfrac{\partial |V|^2/2}{\partial x_j}\right]+\dfrac{\partial \tau_{ji}V_i}{\partial x_j}+S_h \\[2ex]
\dfrac{\partial(\rho \alpha_i)}{\partial t}+\dfrac{\partial}{\partial x_j}(\rho V_j \alpha_i)=\dfrac{\partial}{\partial x_j}\left[\left(\dfrac{\mu}{Sc}+\dfrac{\mu_t}{Sc_t}\right)\dfrac{\partial \alpha_i}{\partial x_j}\right]+S_i \\[2ex]
\dfrac{\partial(\rho k_t)}{\partial t}+\dfrac{\partial}{\partial x_j}(\rho V_j k_t)=\dfrac{\partial}{\partial x_j}\left[\left(\mu+\dfrac{\mu_t}{\sigma_k}\right)\dfrac{\partial k_t}{\partial x_j}\right]+\rho(P_k-\varepsilon) \\[2ex]
\dfrac{\partial(\rho \varepsilon)}{\partial t}+\dfrac{\partial}{\partial x_j}(\rho V_j \varepsilon)=\dfrac{\partial}{\partial x_j}\left[\left(\mu+\dfrac{\mu_t}{\sigma_\varepsilon}\right)\dfrac{\partial \varepsilon}{\partial x_j}\right]+\rho\dfrac{\varepsilon}{k_t}\left(C_1 P_k-C_2\varepsilon+C_3\dfrac{P_k^2}{\varepsilon}\right)
\end{array}
\right\}
$$

Numerical Approach

- Numerical Scheme: Predictor plus correctors 2nd-order time marching scheme with TVD shock capturing limiter for the convection terms and central scheme for other terms of the transport equations
- VLES (Very Large-Eddy Simulation) based on the extended 2-eq turbulence model (Chen & Kim, 1987)

$$\hat{\mu}_t = \rho\, C_\mu \frac{\hat{k}^2}{\hat{\varepsilon}}$$

where

$$\hat{\varepsilon} = \varepsilon$$

$$\hat{k} = k\left\{1 - f\left(\frac{\delta}{\ell}\right)\right\}$$

and

$$f\left(\frac{\delta}{\ell}\right) = \begin{cases} 1-\left(\frac{\delta}{\ell}\right)^{2/3} & for \quad \delta < \ell \\ 0 & for \quad \delta \geq \ell \end{cases}$$

where

$$\delta = \beta \max\left[h\,,\,|u|\Delta t\right], \quad h = (cell\ volume)^{1/3}, \quad \beta = 2 \sim 5$$

$$\ell = \frac{k^{3/2}}{\varepsilon} \quad , i.e.\ Kolmogorov\ length\ scale$$

Numerical Approach

- Real-fluid thermodynamics properties for O_2, H_2, N_2, N_2O, H_2O_2+water, RP-1, etc.
- HBMS equations of state: (Hirschfelder, Buehler, McGee, Sutton)

Thermal equation of state:

$$\frac{p}{p_c} = \sum_{j-1}^{4} T_r^{j-2} \sum_{i=1}^{6} B_{ij} \rho_r^{i-2} \quad ; \quad T_r = \frac{T}{T_c} \quad ; \quad \rho_r = \frac{\rho}{\rho_c}$$

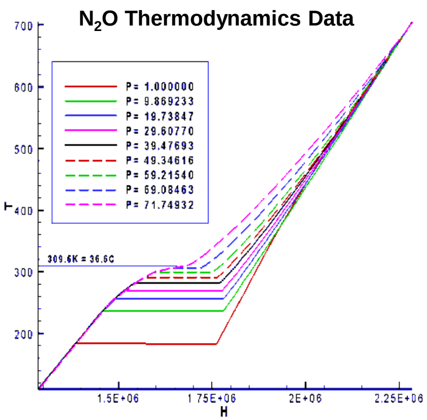

Carolic equation of state:

$$\frac{H - H_c}{RT} = Z_c \int_0^{\rho_r} \left[\frac{p}{T_r} - \left(\frac{\partial p}{\partial T_r} \right)_{\rho_r} \right] \rho_r^{-2} d\rho_r + Z_c \frac{p}{\rho_r T_r} - 1$$

ρ_c: critical density, Z_c: compressibility at the critical condition

H: real-fluid enthalpy, H_0: ideal-gas enthalpy

B_{ij}: coefficients of the thermal property polynomial

Numerical Approach

O_2

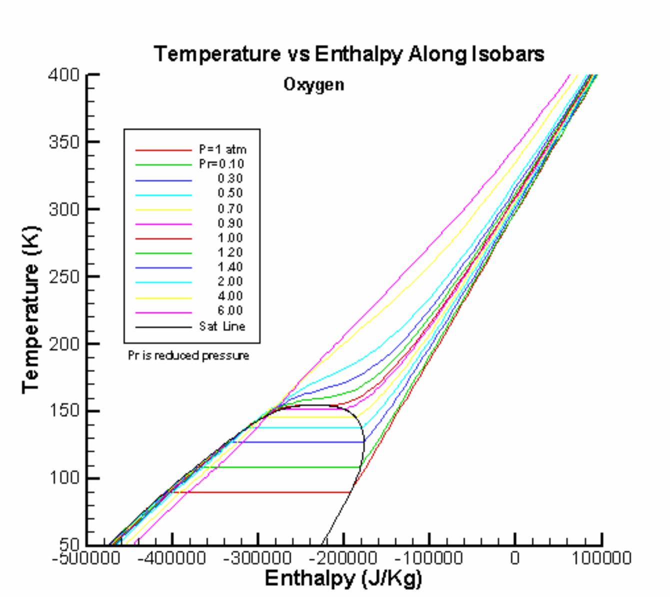

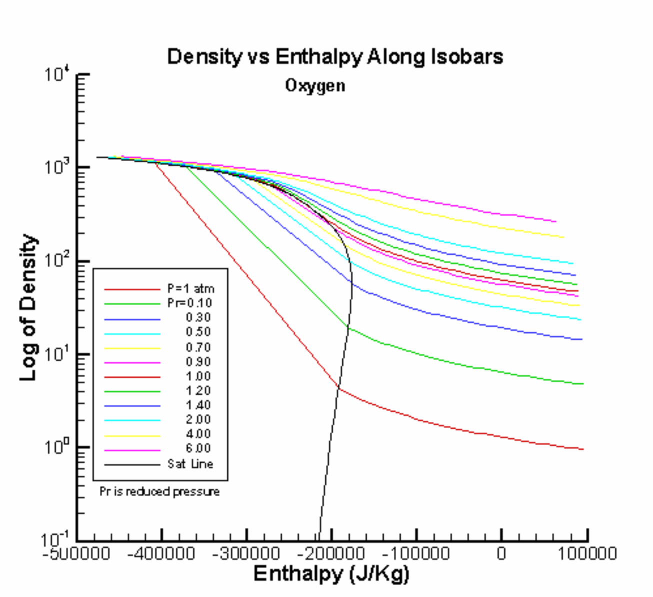

H_2

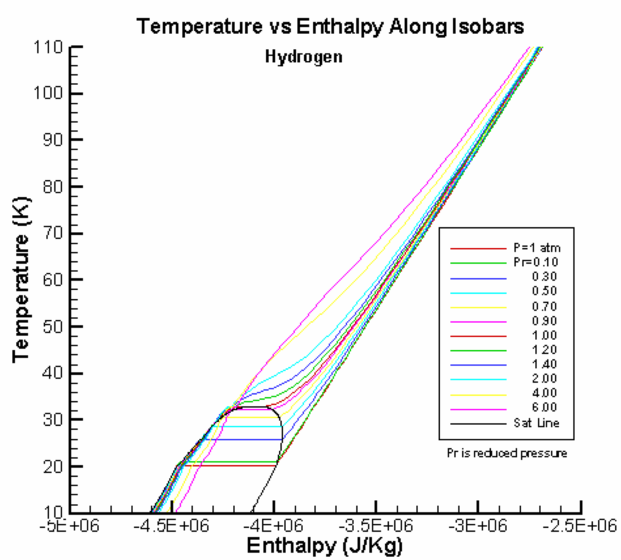

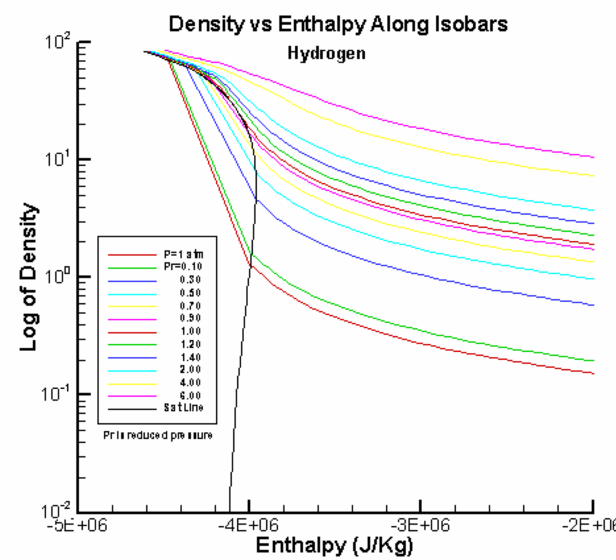

Numerical Approach

N_2

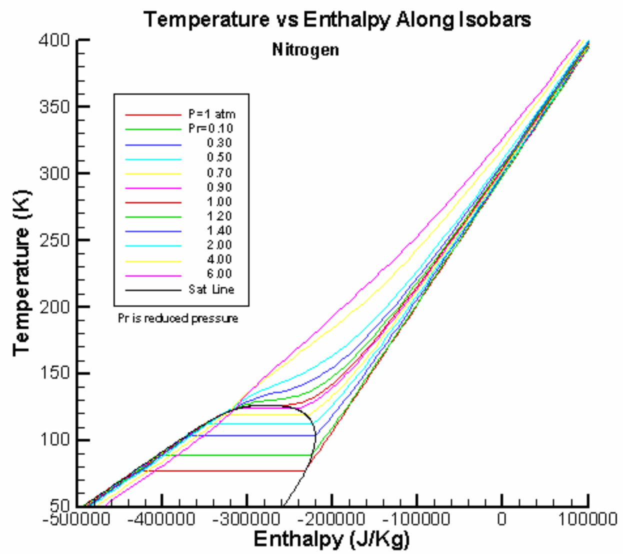

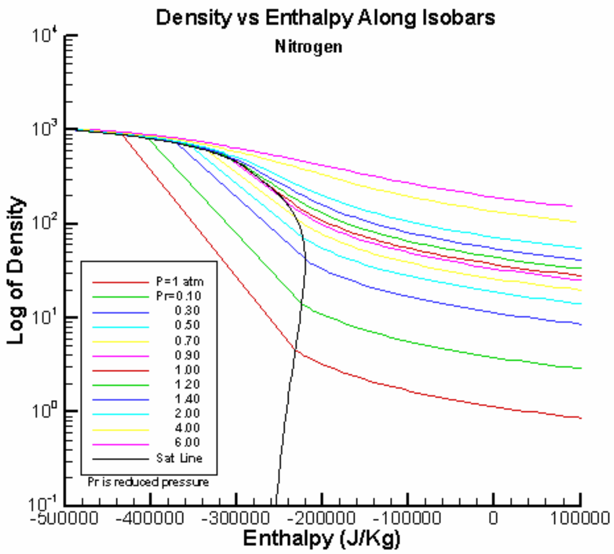

RP-1

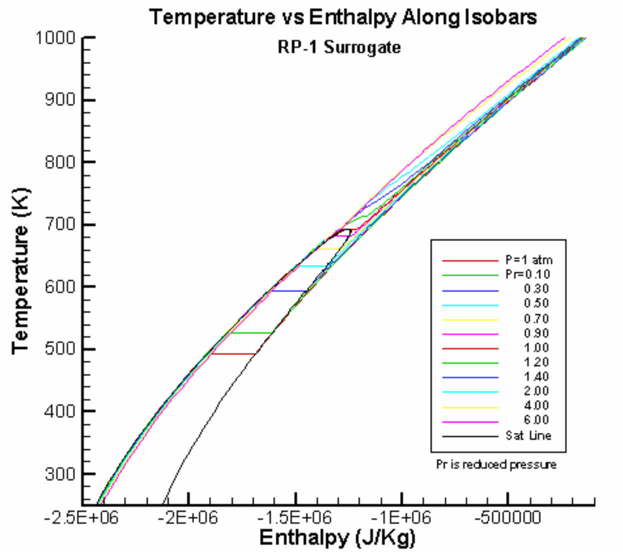

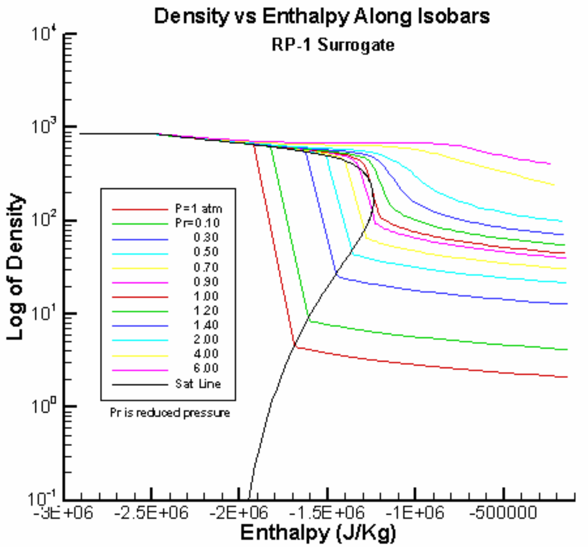

Numerical Approach

- Reacting flow model: finite-rate chemistry with point-implicit

Liquid: LOX-LH_2

8 Species, 9 Reactions

Liquid: LOX-PR-1

10 Species, 17 Reactions, with soot formation

Hybrid: N_2O-HTPB

16 Species: C_4H_6, C_2H_4, O_2, H_2O, O, H, OH, HO_2, H_2, CO, CO_2, N, N_2, N_2O, NO, NO_2

29 Reactions:

Grain Surface Global Reaction: HTPB $\rightarrow$ 0.7 C_4H_6 + 0.3 C_2H_4			
Gas-Phase Reactions:			
1	$C_4H_6 + O_2 \rightarrow 2\,CO + C_2H_4 + H_2$	16	$2N + M = N_2 + M$
2	$C_2H_4 + O_2 \rightarrow 2\,CO + 2\,H_2$	17	$CO + OH = CO_2 + H$
3	$O_2 + H_2 = 2\,OH$	18	$CO + O_2 = CO_2 + O$
4	$H_2 + OH = H_2O + H$	19	$O + CO + M = CO_2 + M$
5	$2\,OH = H_2O + O$	20	$N + NO = N_2 + O$
6	$H_2 + O = H + OH$	21	$N + O_2 = NO + O$
7	$O_2 + H = O + OH$	22	$N + OH = NO + H$
8	$O + H + M = OH + M$	23	$N_2O + O = N_2 + O_2$
9	$2\,O + M = O_2 + M$	24	$N_2O + O = 2\,NO$
10	$2\,H + M = H_2 + M$	25	$N_2O + H = N_2 + OH$
11	$H + OH + M = H_2O + M$	26	$N_2O + OH = N_2 + HO_2$
12	$H + O_2 + M = HO_2 + M$	27	$N_2O + M = N_2 + O + M$
13	$H + HO_2 = 2\,OH$	28	$HO_2 + NO = NO_2 + OH$
14	$H + HO_2 = H_2 + O_2$	29	$NO + O = NO_2$
15	$OH + HO_2 = H_2O + O_2$		

Hybrid: H_2O_2-HTPB

12 Species: C_4H_6, C_2H_4, O_2, H_2O, O, H, OH, HO_2, H_2, CO, CO_2, H_2O_2

27 Reactions:

Grain Surface Global Reaction: HTPB $\rightarrow$ 0.7 C_4H_6 + 0.3 C_2H_4			
Gas-Phase Reactions:			
1	$C_4H_6 + O_2 \rightarrow 2\,CO + C_2H_4 + H_2$	15	$OH + HO_2 = H_2O + O_2$
2	$C_2H_4 + O_2 \rightarrow 2\,CO + 2\,H_2$	16	$CO + OH = CO_2 + H$
3	$O_2 + H_2 = 2\,OH$	17	$CO + O_2 = CO_2 + O$
4	$H_2 + OH = H_2O + H$	18	$O + CO + M = CO_2 + M$
5	$2\,OH = H_2O + O$	19	$O + OH + M = HO_2 + M$
6	$H_2 + O = H + OH$	20	$H + HO_2 = H_2O + O$
7	$O_2 + H = O + OH$	21	$O + HO_2 = OH + O_2$
8	$O + H + M = OH + M$	22	$H_2O_2 + M = 2\,OH + M$
9	$2\,O + M = O_2 + M$	23	$2\,HO_2 = H_2O_2 + O_2$
10	$2\,H + M = H_2 + M$	24	$H_2O_2 + H = H_2 + HO_2$
11	$H + OH + M = H_2O + M$	25	$H_2O_2 + H = H_2O + OH$
12	$H + O_2 + M = HO_2 + M$	26	$H_2O_2 + O = O_2 + H_2O$
13	$H + HO_2 = 2\,OH$	27	$H_2O_2 + O = OH + HO_2$
14	$H + HO_2 = H_2 + O_2$		

Numerical Approach

- Fluid-structure interaction modeling:
  1. Flow Solver
  2. Structural Dynamics Solver
     - Aeroelastic Equation of Motion

       $$[M]\{\ddot{Y}\}+[C]\{\dot{Y}\}+[K]\{Y\}=\{F\}$$

     - Generalized Transformation

       $$\{Y\}=[\Phi]\{Z\};\ \{\dot{Y}\}=[\Phi]\{\dot{Z}\};\ \{\ddot{Y}\}=[\Phi]\{\ddot{Z}\}$$

     - Generalized Equation of Motion (Rayleigh Damping Assumed)

       $$\{\ddot{Z}\}+[\Phi]^T[C][\Phi]\{\dot{Z}\}+[\Phi]^T[K][\Phi]\{Z\}=[\Phi]^T\{F\}$$

     - N equations are solved for N structural modes
  3. Boundary Displacement and Moving-Grid Re-meshing
  4. Iterative Close Coupling for Each Time Step

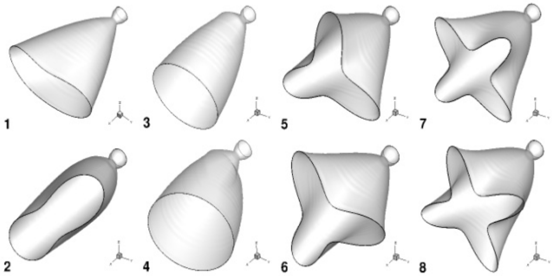

Numerical Model Validations

- Transient flow simulations:

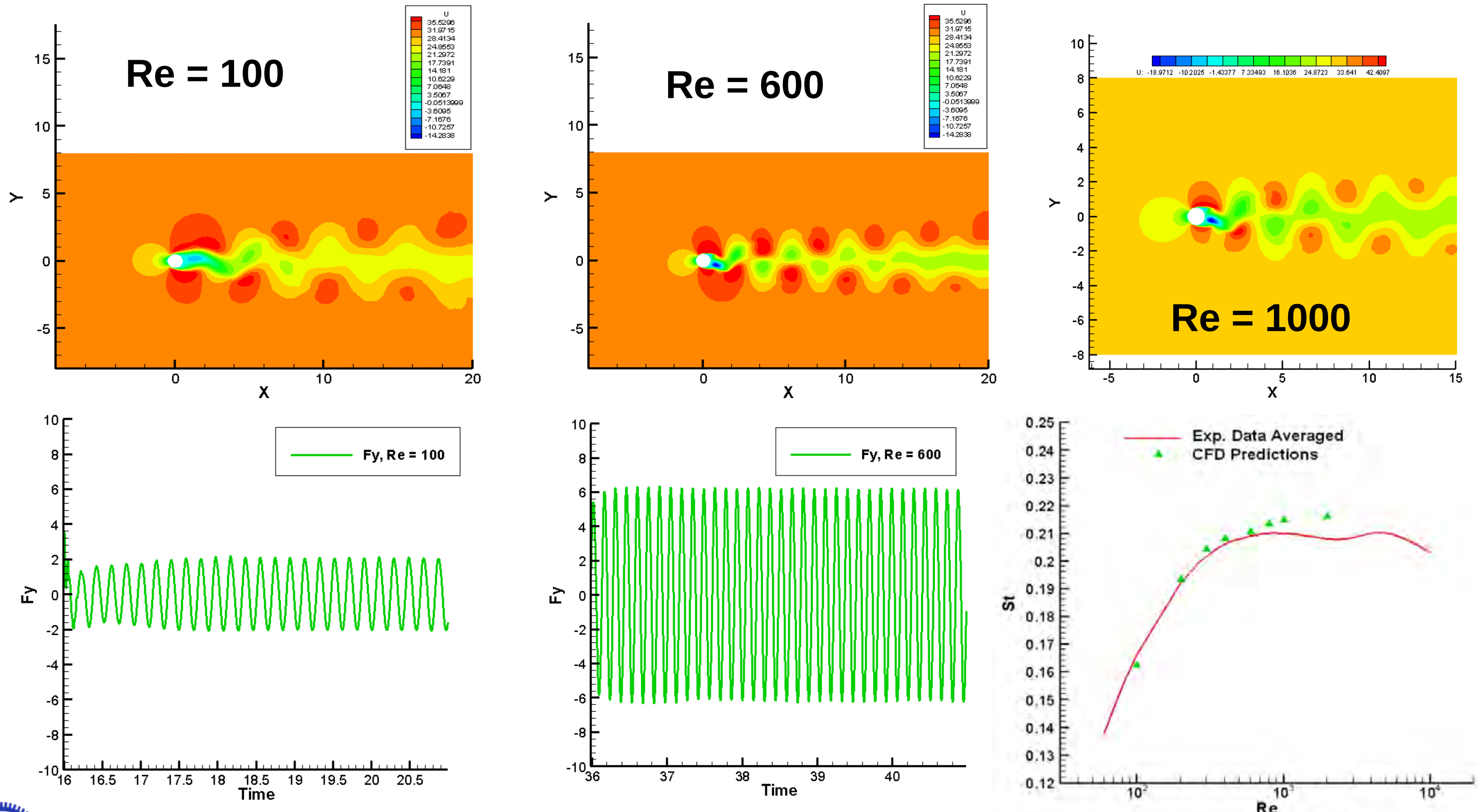

Numerical Model Validations

- Reacting Hot Flow, Re = 350
- 6 Species, 9 Reactions

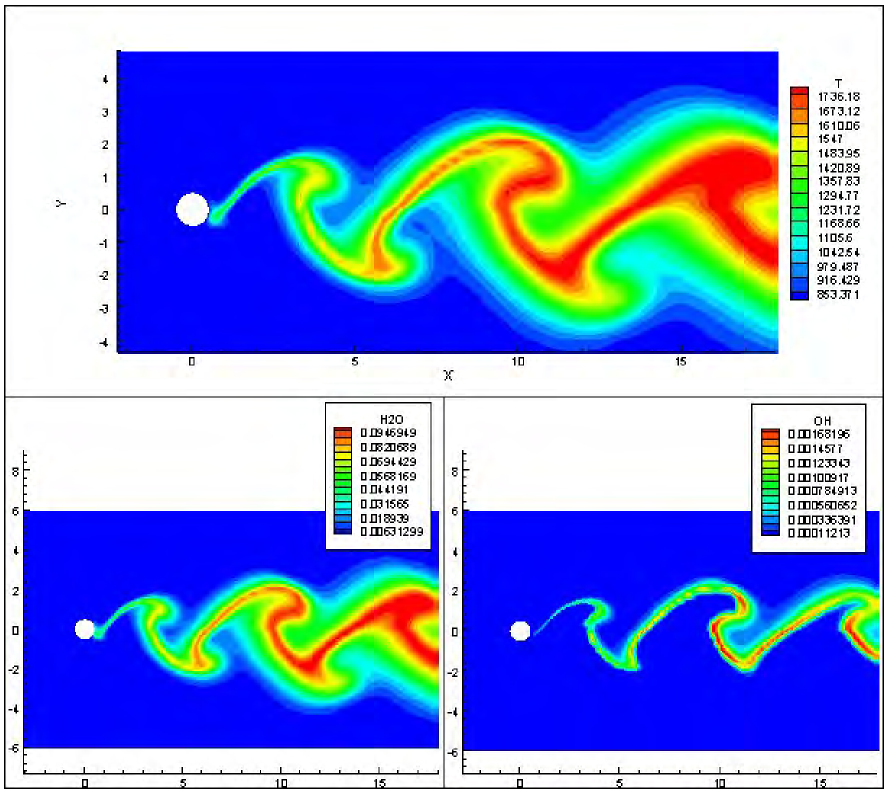

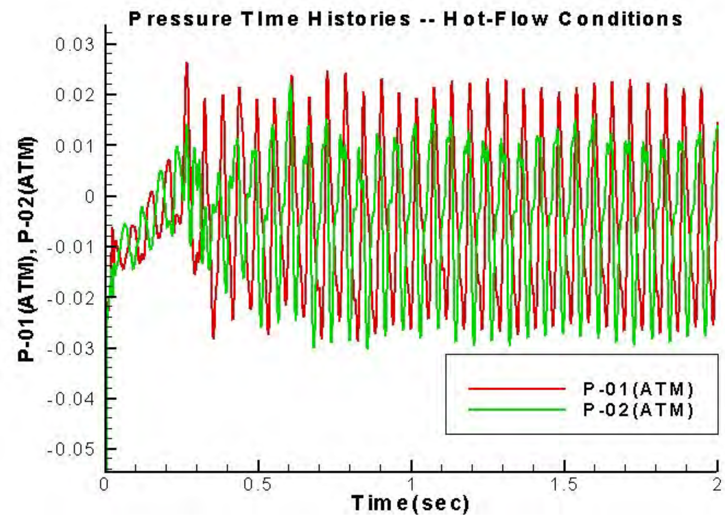

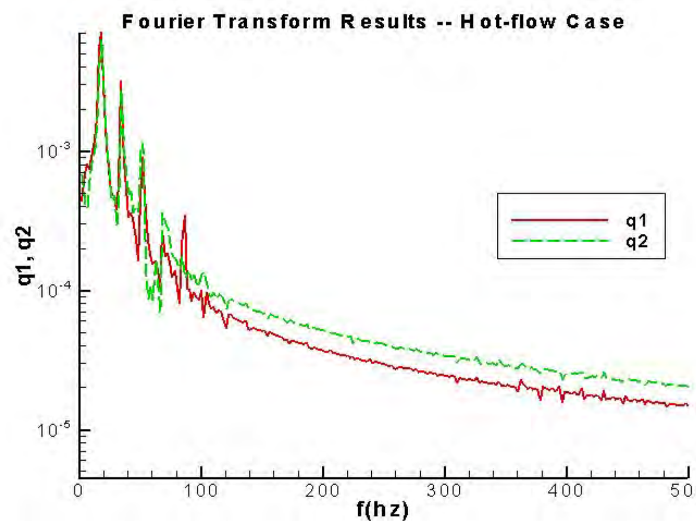

Numerical Model Validations

- Mascotte RCM-2 LOX/GH2 Combustion (DLR, 2001)
- Predicted Flame Shape closely resembles Abel-Transformed Emission Image from Experiment

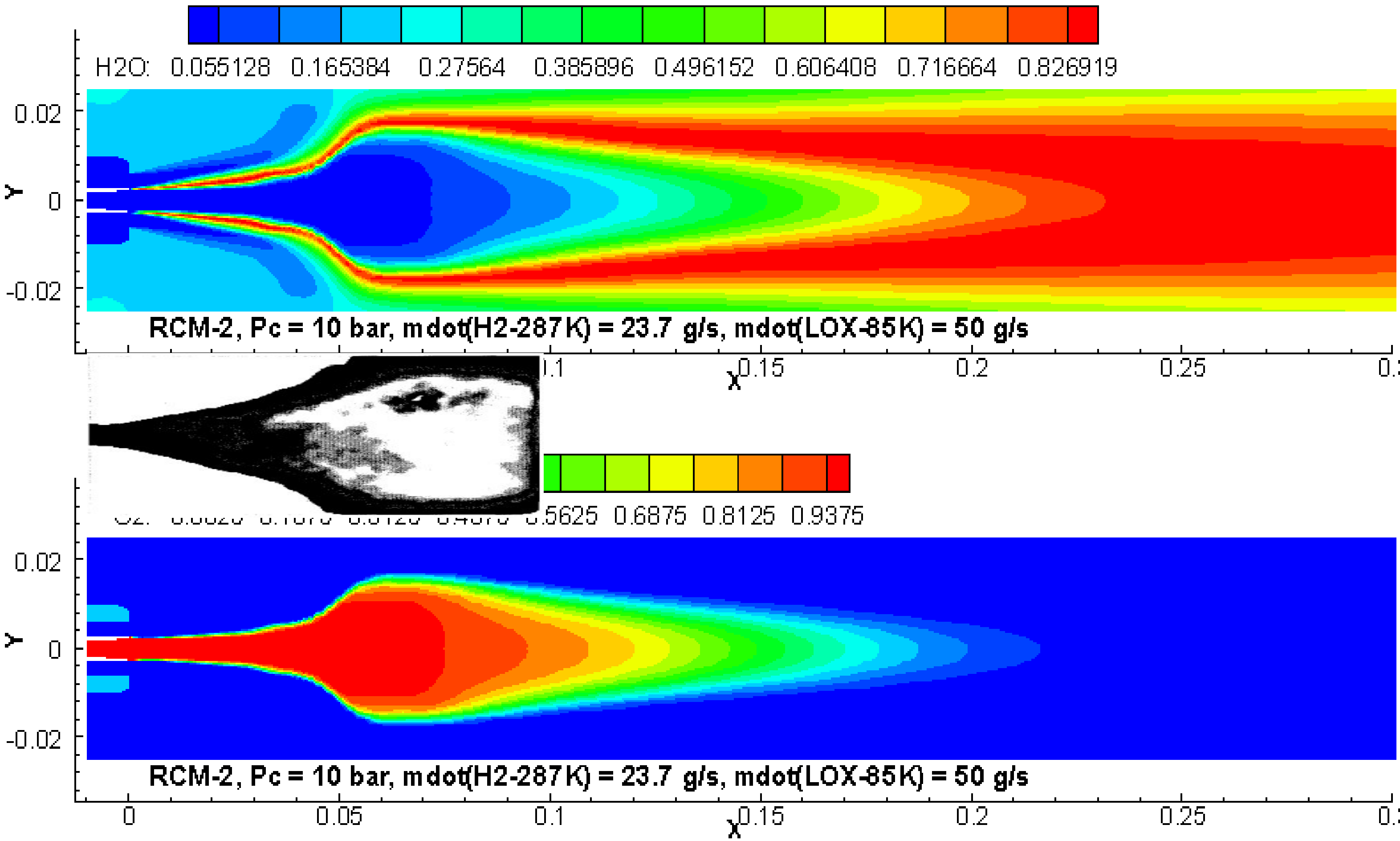

Numerical Model Validations

- Start-up Transient Flow Simulations for J-2X and SSME Engines
- FSS and RSS Patterns and Side Forces Predicted
- Fluid-Structure Interaction Simulated

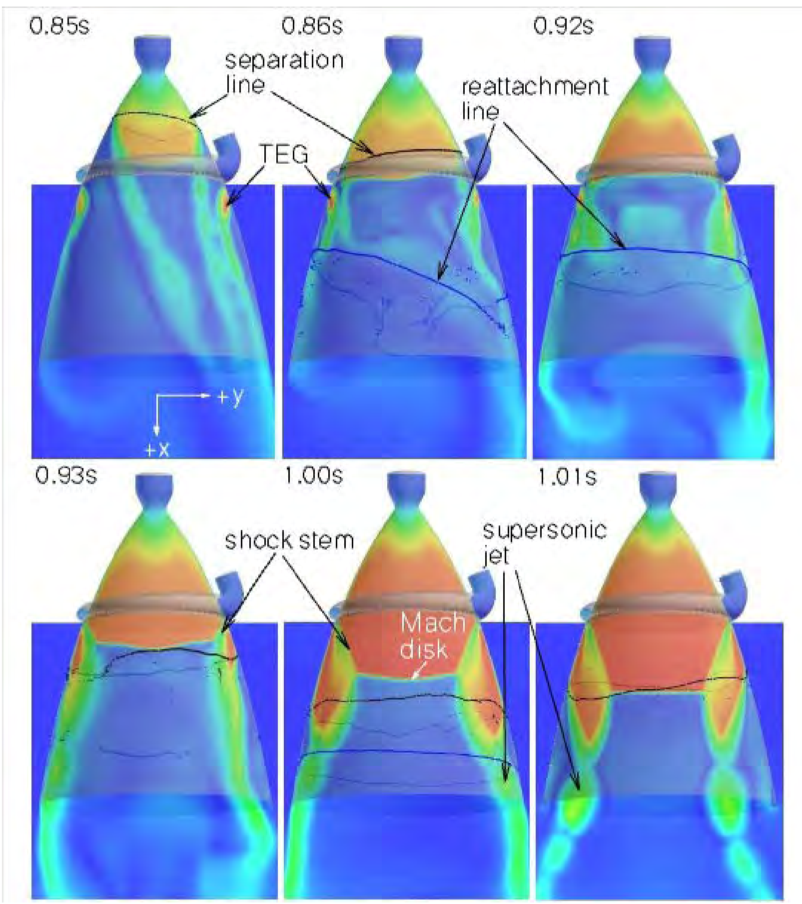

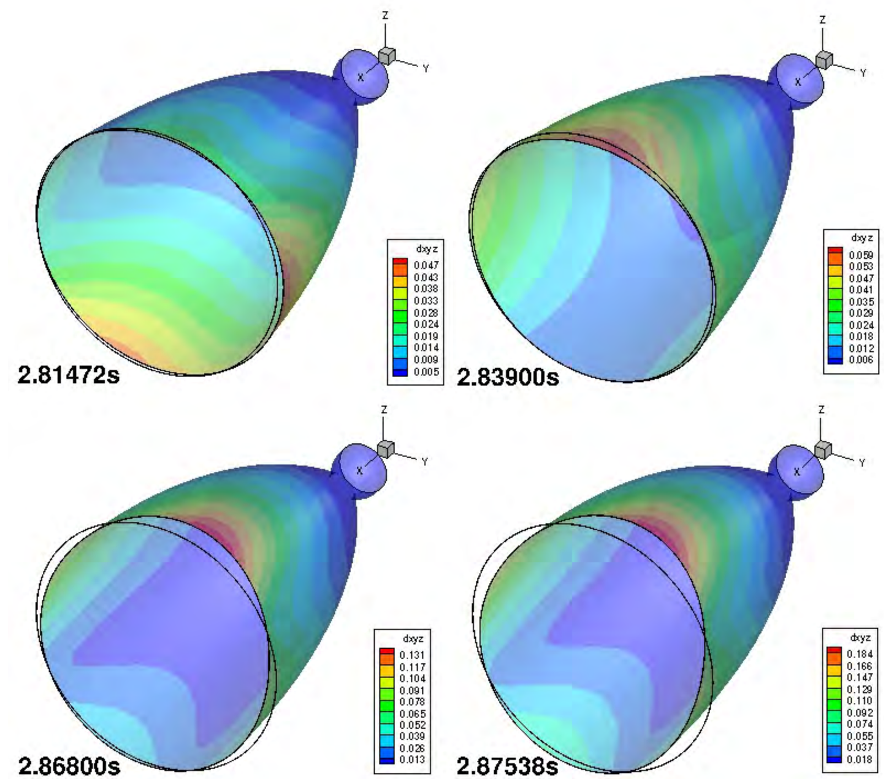

Rocket Engine Design Applications

- Hybrid Rocket Engine Development
  - Axial Single Port with Mixing Enhancers Design Cases

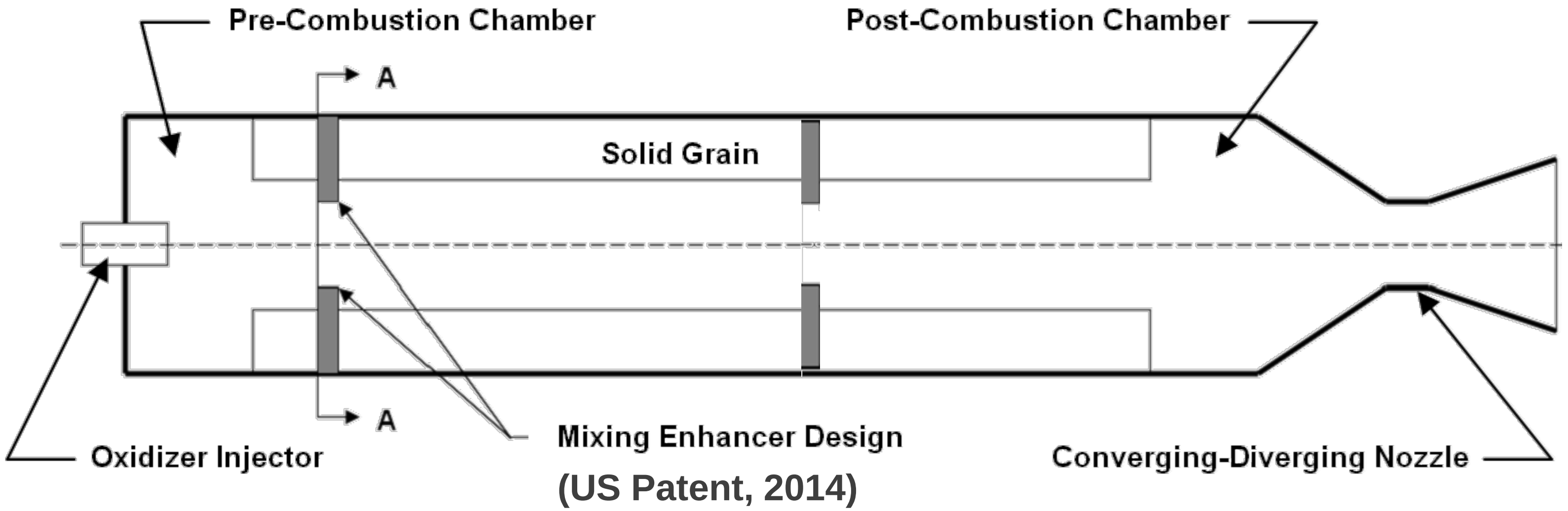

- 300 and 1000 kgf Thrust Levels Hybrid Combustion Chamber design with a Pintle Injector
- N_2O Oxidizer and HTPB Solid Fuel which decomposes into roughly 70% C_4H_6 and 30% C_2H_4
- Single and multiple rows of Mixing Enhancers
- Number of computational cells: 5.2 millions

Rocket Engine Design Applications

- Hybrid Rocket Engine Development

Throat diameter: 56 mm
Expansion ratio: 7

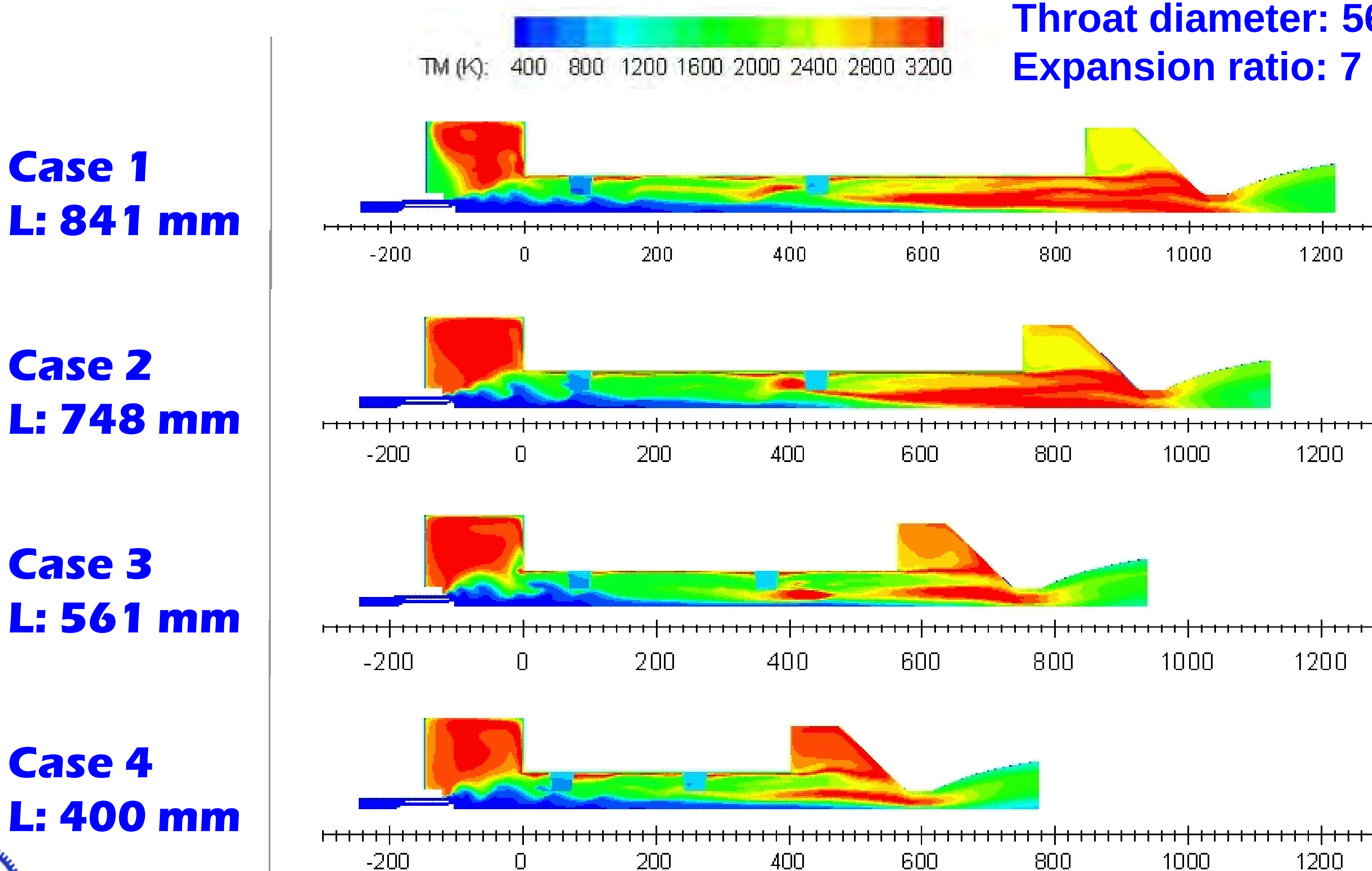

L: Port Length

Rocket Engine Design Applications

- Hybrid Rocket Engine Development

	Chamber Pressure (bar)	Thrust (kgf)	ISP (sec)	Mass Flow Rate (kg/sec)	C* (m/s)	O/F Ratio
Case 1 L841 mm	28.07	1124.9	256	4.39	1579.0	8.13
Case 2 L748 mm	28.44	1126.2	257	4.38	1604.3	8.38
Case 3 L561 mm	27.96	1122.0	258	4.35	1589.2	12.49
Case 4 L400 mm	27.69	1112.9	245	4.54	1506.8	16.58

Rocket Engine Design Applications

- Hybrid Rocket Engine Development
  - Baseline single-port design:
    - Vacuum Isp of experiment = 187.2 s
    - Calculated vacuum Isp = 191.4 s (2-D), 190.8 s (3-D)
  - Modified design with 1-stage mixing enhancers:
    - Vacuum Isp of experiment = 222.2 s
    - Calculated vacuum Isp = 223.8 s (3-D)
  - 1000 kgf design with 2-stage mixing enhancers:
    - Vacuum Isp of experiment = 256.5 s (748 mm Port Length)
    - Calculated vacuum Isp = 257.3 s (3-D)

Rocket Engine Design Applications

- Hybrid Rocket Engine Development
  - Cases Investigated:
    - Base line dual vortical-flow chamber model
    - Oxidizer injection systems
    - Upper-stage high-altitude hybrid rocket propulsion for 700 kgf, 1,000 kgf and 4,500 kgf thrust levels
    - Dual and quad vortical-flow chambers

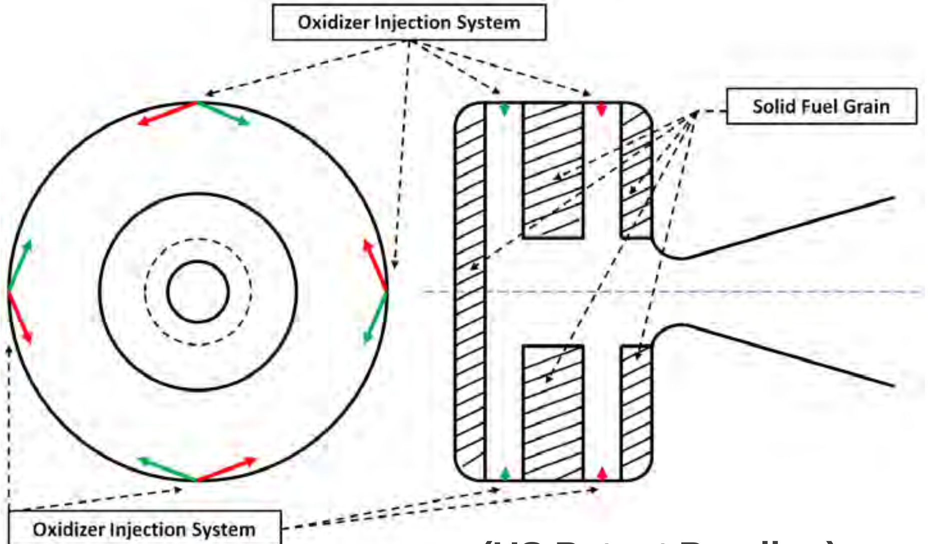

(US Patent Pending)

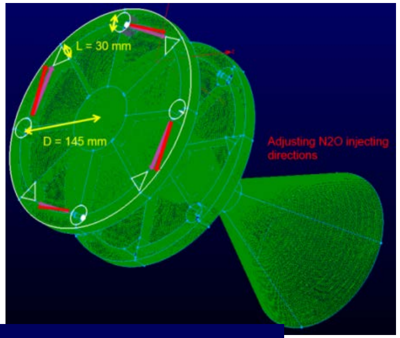

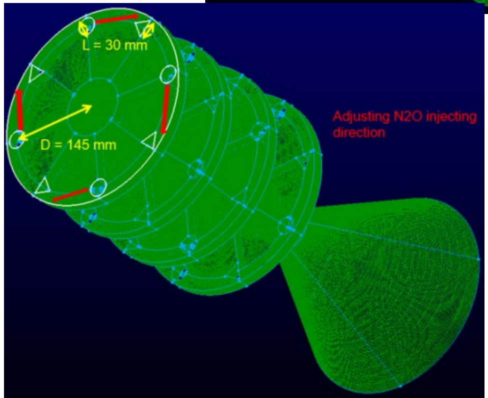

Rocket Engine Design Applications

- Hybrid Rocket Engine Development
  - Stream traces show the effects of increased residence time along the HTPB surfaces
  - High flow turning and counter-rotation high shear stress effects

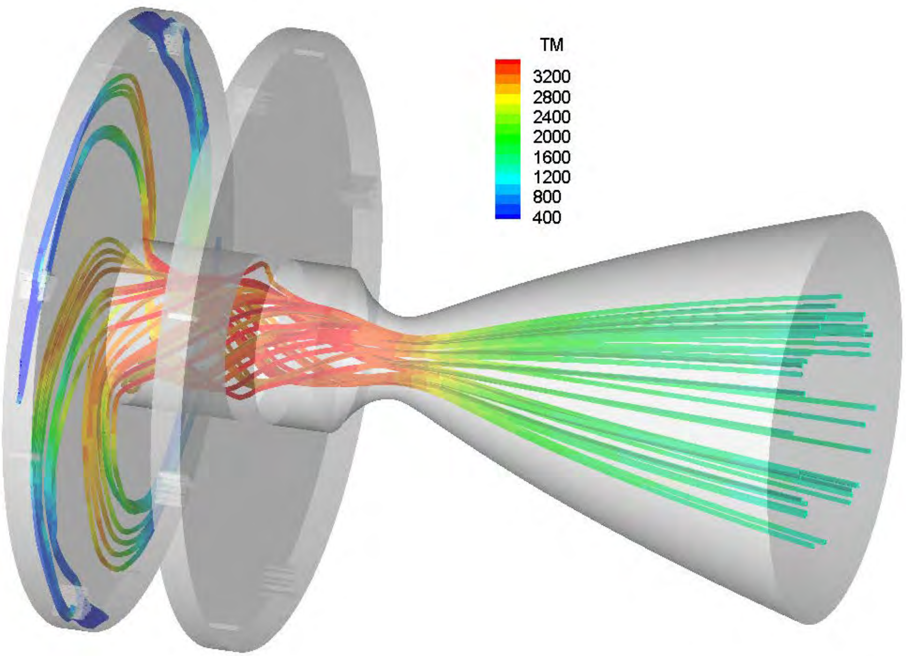

Fwd-Disk-Chamber Stream Traces

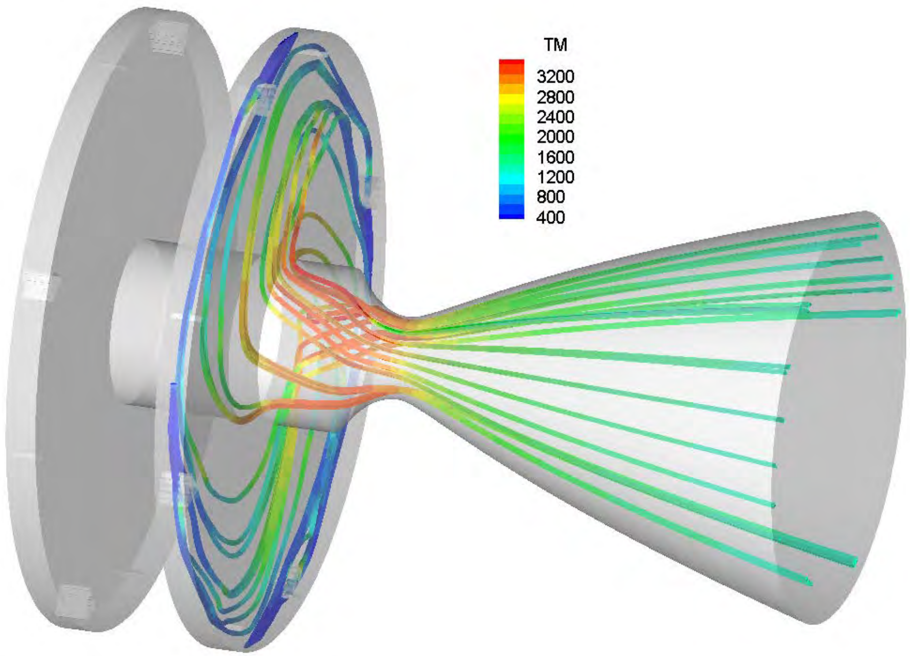

Aft-Disk-Chamber Stream Traces

Rocket Engine Design Applications

- Hybrid Rocket Engine Development
  - Summary of different thrust level cases (nozzle expansion area ratio of 25)
  - O/F ratios are on the high side due to low regression rate of HTPB
  - Vacuum Isp around 291~292 sec for these cases
  - Indicating overall combustion efficiency over 0.95 (Theoretical vacuum Isp for these cases is 305 sec)

Thrust (N / Kgf)	N_2O Flow Rate (kg/s)	HTPB Flow Rate (kg/s)	O/F	Vacuum Isp (sec)
7096.9 / 724.2	2.2646	0.2217	10.2	291.3
10,706.2 / 1092.5	3.4258	0.3143	10.9	292.1
44,754.5 / 4,566.7	14.3977	1.2739	11.3	291.4

Rocket Engine Design Applications

- Hybrid Rocket Engine Development
  - Performance comparisons of dual-vortical-flow and quad-vortical-flow chambers (nozzle expansion = 23)

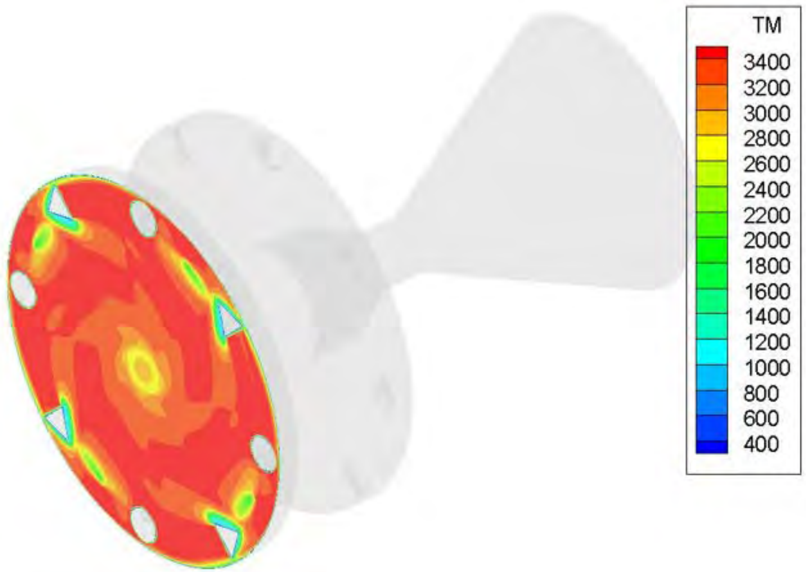

Dual-Vortical-Flow Chamber

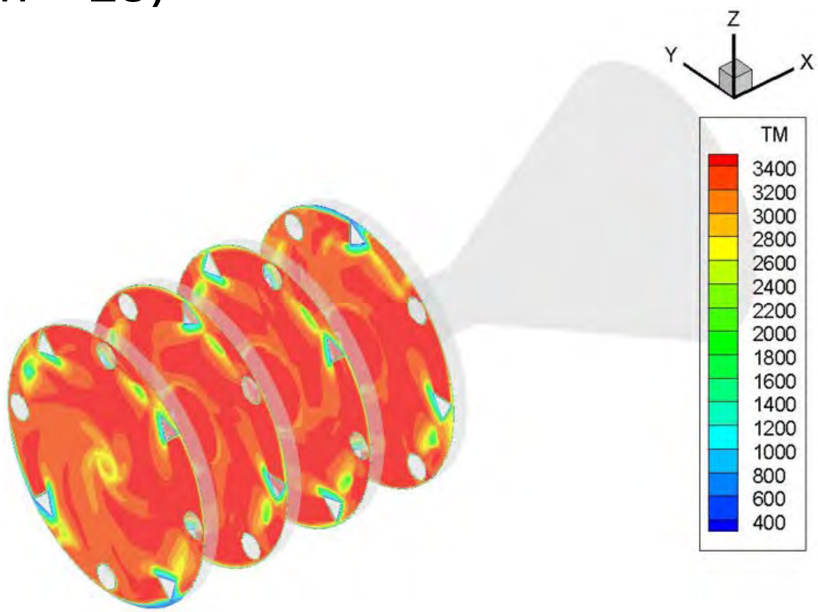

Quad-Vortical-Flow Chamber

Chamber Design	Thrust (kgf)	Propellant Flow Rate (kg/sec)	O/F	Vacuum Isp (sec)	C* (m/sec)
DVF	1,146.7	4.00	9.48	286	1653.37
QVF	2,299.4	7.99	9.67	288	1681.86

Rocket Engine Design Applications

- Dual-vortical-flow designs provide good thrust performance for HTPB hybrid Systems

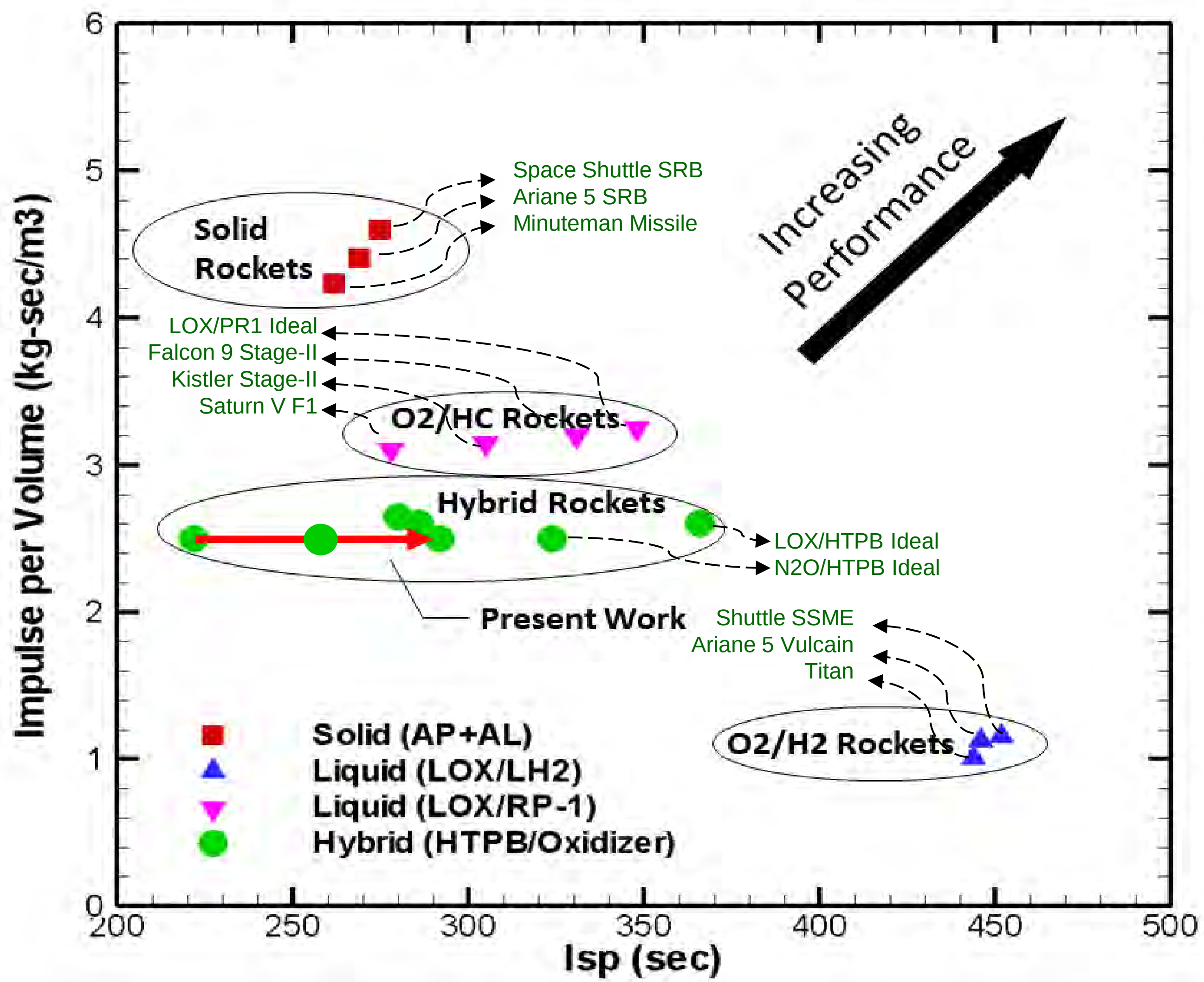

Rocket Engine Design Applications

- Hybrid Rocket Engine Development

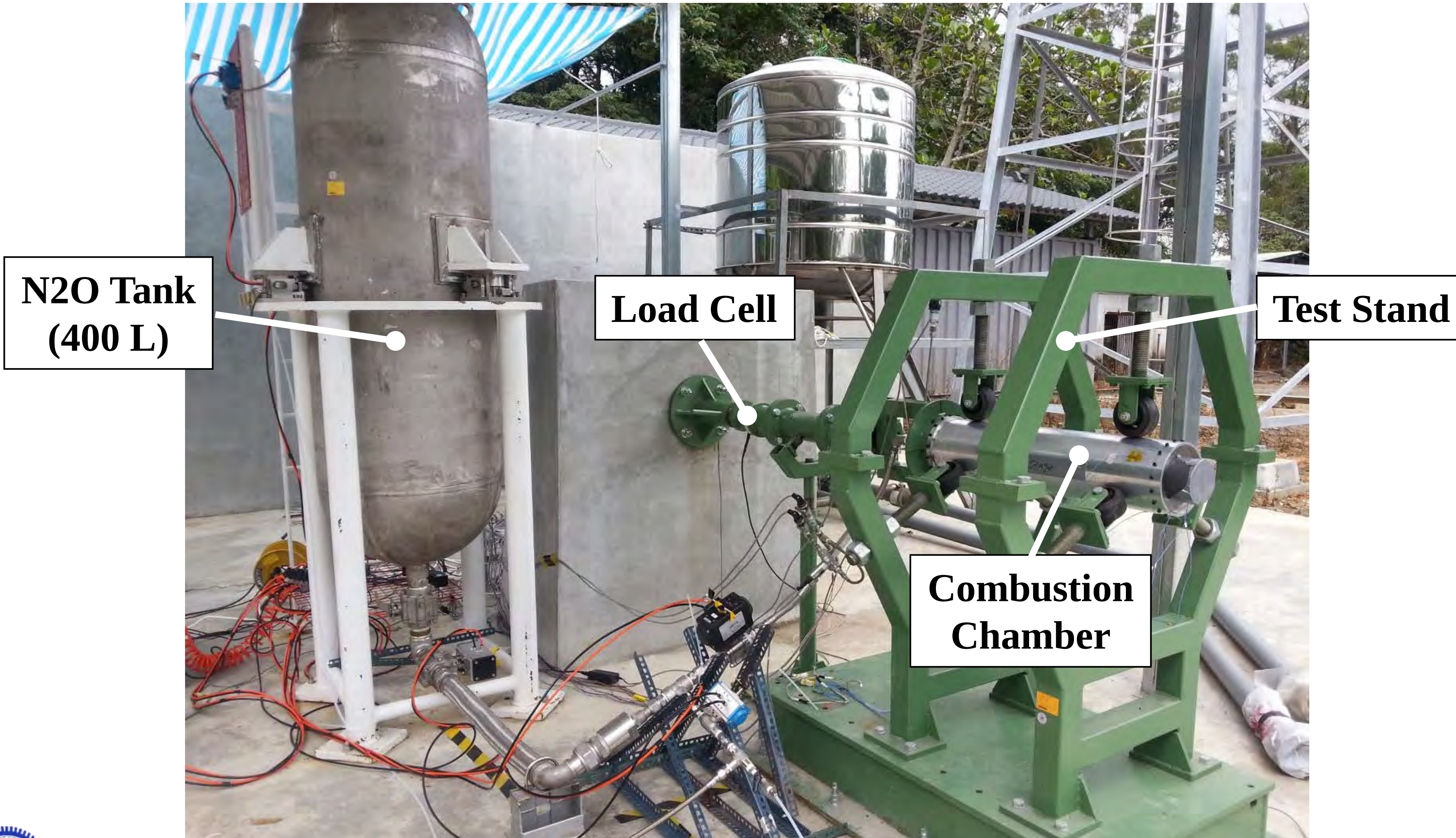

Rocket Engine Design Applications

Conclusions

- A multiphysics CFD model is presented with benchmark validations for liquid and hybrid rocket design applications
- Real-fluid property model has been demonstrated to be very important in accurate descriptions of the combustion physics in rocket propulsion systems
- Fluid-structure interaction modeling for rocket engine start-up and shutdown transients will provide more realistic simulations
- Application of the present model in hybrid rocket engine developments has shown cost-effective designs for improving combustion efficiency and the overall thrust performance

Acknowledgments

- This work is supported by the Sounding Rocket Program of the National Space Organization, National Applied Research Laboratory and the Advanced Rocket Research Center of National Chiao Tung University, Taiwan
- The computational resources and services are provided by the National Center for High-performance Computing, the National Applied Research Laboratory, Taiwan

THE END

Thanks for your attention

Rocket Engine Design Applications

Hybrid Engine Hot-Fire and Flight Test
(1000 kgf Thrust Level)